



REGULAR ARTICLE

New self-assembled archetypes in crown ether substituted Δ^Z Phe containing tripeptides

KALPANA TOMAR and GURUNATH RAMANATHAN*

Department of Chemistry, Indian Institute of Technology Kanpur, Kanpur, Uttar Pradesh 208016, India
E-mail: gurunath@iitk.ac.in

MS received 17 October 2018; revised 4 February 2019; accepted 18 March 2019

Abstract. We examine the effect of crown ether ring sizes on structure and properties of three terminally protected tripeptides containing substituted dehydrophenylalanine residues; Bz- Δ Phe(12-crown-4)-Phe-Phe-OMe, Bz- Δ Phe(15-crown-5)-Phe-Phe-OMe, Bz- Δ Phe(18-crown-6)-Phe-Phe-OMe. The resultant self-assembly of the peptides generates nano-vesicles, which further alter into the necklace type of structures that were characterized *via* their SEM, LRTEM, and AFM images. We also report the disruption of these vesicles in the presence of different metal ions.

Keywords. Crown ethers peptides; dehydrophenylalanine peptides; self-assembly; metal binding peptides.

1. Introduction

Crown ethers are a class of macrocycles that possess an uncanny ability to form metal complexes with the alkali and alkaline earth metals, lanthanides, and transition metal ions. They have been widely applied in the construction of molecular sensors as well as in the design of ion-selective ligands using host-guest chemistry. Interestingly, the modulation in the size of crown ether rings enhances the sensing ability of these molecules to specific metal ions. Crown ethers and their derivatives are also known to form ordered structures. For instance, crown ether substituted with Phthalocyanine can self-assemble into well-defined superhelical structures.¹ Also, Voyer and coworkers have integrated crown ethers into dihydroxyphenylalanine side chains to produce substituted peptides.² Phe-Phe based peptides have also shown diverse self-assembled morphologies such as nanofiber, nanotubes, nanovesicles, micelles, nanoribbons, etc.³ Recently, crown ether containing peptides have been explored in the biological applications. These applications include an ability to regulate enzyme activity, interact with or cleave DNA, and act as antimicrobial agents.⁴ Several researchers have used crown ether containing peptides in the preparation of receptors, enzyme mimics, artificial ion channels, and dendrimers.^{5a, 4a, 5b, 4b, 1}

Considering the potential advantages of the crown ethers and Phe-Phe motif-based peptides, we have synthesized the applications of the crown ether containing peptides. Here, crown ether containing tripeptides were reported, namely P-12C4: Bz- Δ Phe(12-crown-4)-Phe-Phe-OMe, P-15C5: Bz- Δ Phe(15-crown-5)-Phe-Phe-OMe, and P-18C6: Bz- Δ Phe(18-crown-6)-Phe-Phe-OMe (Figure 1). These tripeptides contained a Phe-Phe motif and Δ^Z Phe residue with different crown rings. Additionally, we also explored the metal sensing ability of these peptides. Interestingly, these crown-ether containing tripeptides turned out to be promising lead candidates for Hg²⁺ ion sensing. The microscopic studies of the soft structures formed by these molecules have demonstrated various nano-vesicular morphologies which could rupture in the presence of Hg²⁺ and Na⁺ ions.

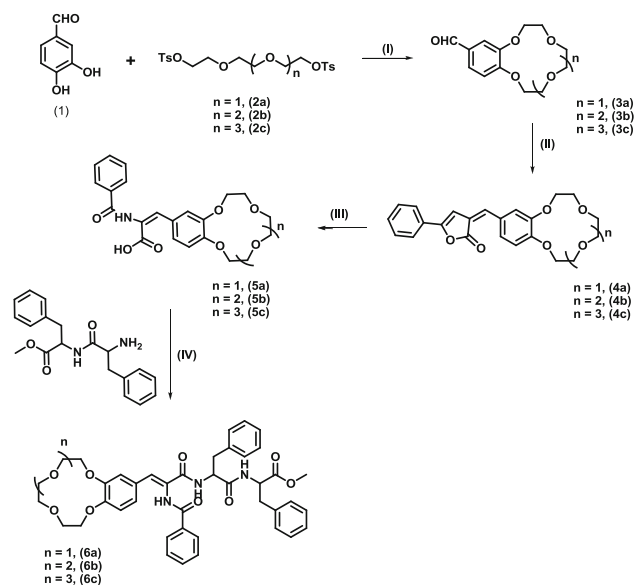
2. Materials and methods

2.1 Material

All amino acids barring Δ Phe were of *L*-configuration. The amino acids were procured from commercial sources. IR spectra and CD spectra of peptides were recorded on Perkin Elmer spectrometer version 10.03.06 FT-IRTM and JASCO-

*For correspondence

Electronic supplementary material: The online version of this article (<https://doi.org/10.1007/s12039-019-1623-8>) contains supplementary material, which is available to authorized users.



Scheme 1. Scheme for the synthesis of the tripeptides. (I) $\text{Cs}_2\text{CO}_3/\text{CH}_3\text{CN}$ (II) $\text{CH}_3\text{CO}_2\text{Na}/(\text{CH}_3\text{COO})_2\text{O}$, (III) acetone/1 N NaOH, (IV) DCC/HOBt/DMF.

850 CD Spectropolarimeter respectively. Mass spectra were recorded on Waters ESI-Q tof spectrometer. ^1H NMR spectra of peptides were recorded in JEOL ECS 400 MHz NMR spectrometer using CDCl_3 as a solvent. Absorption spectra measurement was recorded on a Jasco V-550 UV-Visible spectrophotometer, and emission spectra were recorded in a Fluorolog 3.2.1 spectrofluorimeter. AFM samples were imaged with XE70, Park system, South Korea, atomic force microscope and FE-SEM images were recorded with an FEI quanta 200 microscope. TEM samples imaged with FEI tecnai G2 12 twin TEM.

2.2 Peptide synthesis strategy

Peptides were synthesized by solution phase protocol⁶ (Scheme 1). The benzoyl protection was used at *N*-terminus while *C*-terminus had methyl ester protection. Deprotection of Boc (tert-butoxy carbonyl) was performed by 75% TFA (trifluoroacetic acid) in DCM (dichloromethane). Peptides were coupled by using dicyclohexylcarbodiimide (DCC)/1-hydroxy benzotriazole (HOBt). Intermediate peptides were used directly without purification after ascertaining that there was no racemization during the synthesis by high field NMR. The final peptides were purified by column chromatography using a methanol/chloroform gradient. Purified peptides were further characterized by ESI-MS and 400, 500 MHz ^1H NMR in CDCl_3 .

3. Results and Discussion

3.1 Conformational study of tripeptides

To obtain the secondary structure of these three peptides, we recorded Fourier transform infrared (FT-IR), circular

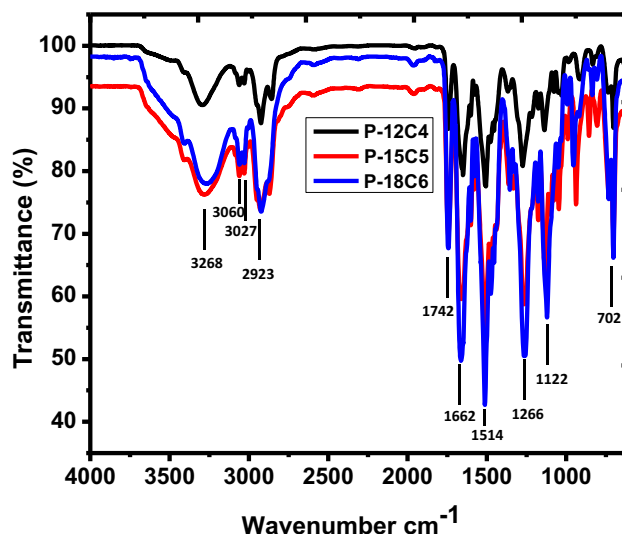


Figure 1. Solid state FT-IR of peptides (recorded as KBr pellet).

dichroism (CD) in solid and solution states. Due to the presence of different functional groups such as CONH, COOCH_3 , aromatic rings, aliphatic groups ($-\text{CH}_2$), etc., the solid-state FT-IR spectrum showed several vibrational bands. The FT-IR bands spectrum for P-18C6 is shown in Figure 1, and the assignments are listed in Table 1.

All peptides show a single amide I peak at 1651 cm^{-1} for P-12C4, 1662 cm^{-1} for P-15C5 and P-18C6 indicating an α -helix turn type conformation. However, characteristic absorption bands in the range of $1610\text{--}1630\text{ cm}^{-1}$ for the aggregated amyloid-like peptides is not observed which suggests that these tripeptides do not aggregate in the solid state.

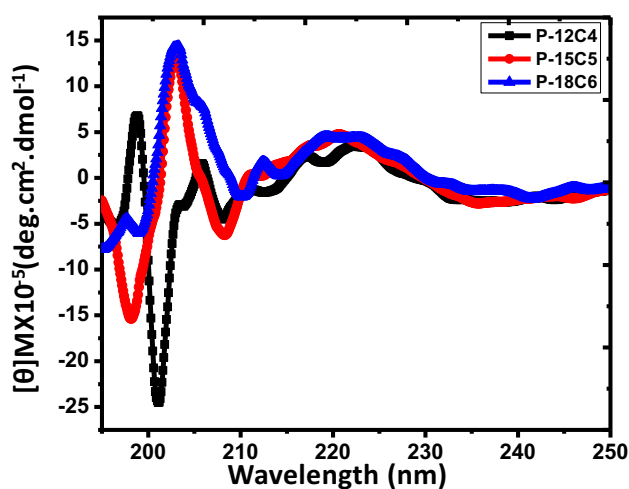
CD spectrum revealed the most preferred conformation of these peptides in solution (Figure 2). While the peptide P-12C4 shows sharp negative peak near 201 nm, P-15C5 and P-18C6 show a sharp negative peak around 198 nm that is diagnostic for a random coil structure.⁷ Persistence of some positive peaks indicates that peptides also have a tendency to adopt other conformations where the geometric arrangement of amide bonds are different from those reported for a random coil structure. The CD spectrum reflects the existence of various types of molecular interactions present in this multi-sized self-assembled structure formed in the solution state.

3.2 Photophysical properties of peptides

To investigate the effect of crown ether on fluorescence properties of peptides, we used $50\text{ }\mu\text{M}$ solution of each of these three peptides in methanol as a solvent. P-12C4 displays an emission band at 403 nm on excitation at 309 nm while P-15C5 and P-18C6 show emission band

Table 1. Assignment of FT-IR bands present in the peptides.

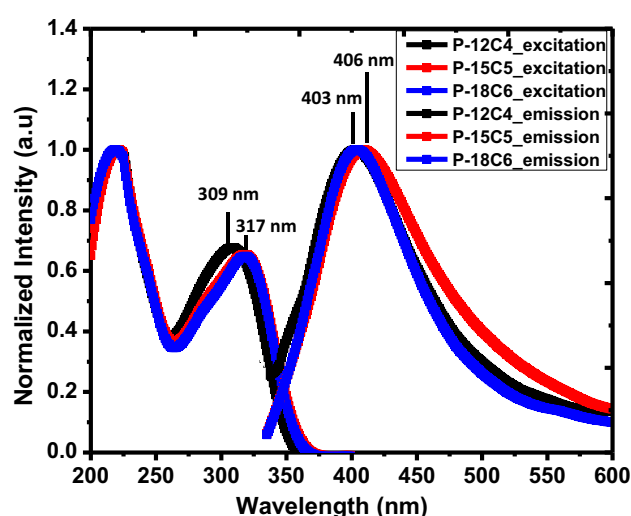
IR frequency (cm ⁻¹)			Modes of assignments
P-12C4	P-15C5	P-18C6	
3295	3280	3268	Amide NH symmetric stretching
3064	3062	3060	NH bending first overtone
3028	3029	3027	Aromatic C-H stretching
2925	2926	2923	-CH ₂ antisymmetric stretching
1743	1742	1742	C=O stretching of the ester
1651	1662	1662	Amide C=O stretching (amide I)
1506	1514	1514	Amide II (NH bend in plane and CN stretch)
1275	1266	1266	Amide III (NH bend in plane and CN stretch)
1140	1126	1122	Ester C-O asymmetric stretch
702	702	702	Out of plane NH bending

**Figure 2.** Circular dichroic spectra of the peptides in methanol (1 mg/mL in 0.1 mm cell).

at 406 and 403 nm, respectively, on excitation at 317 nm (Figure 3). Fluorescence intensity of P-12C4 was lower in comparison to P-15C5 and P-18C6. We have also measured the changes in fluorescence intensity of the peptide in the presence of different metal perchlorate salts. Significant changes in the fluorescence intensity of P-12C4 and P-15C5 were found only in the presence of Hg²⁺ ion (Figures 4, 5). Peptide P-18C6 does not show selectivity for any metal ion, but it does demonstrate a subtle decrease in fluorescence intensity in the presence of copper in comparison to other metal ions (Figure 6). P-15C5, however, shows a marginally better selectivity with mercury in comparison to P-12C4 (Figure 7).

3.3 Morphology and microscopic characterization

For the study of morphological architectures of peptides, we have used 1 mM methanol solutions of each

**Figure 3.** Excitation and emission spectra of peptides (50 μM) in methanol.

of these three peptides when cast on silicon wafers. After a 12 h incubation, the peptides exhibit vesicular structures which could be attributed to the hydrogen bonding and π - π stacking. Moreover, a structural transition of self-assembled material is often commonly observed in the literature.⁸ Both P-12C4 and P-15C5 self-assembled into vesicles with a smooth surface as seen in atomic force microscopy (AFM), scanning electron microscopy (SEM) and low-resolution transmission electron microscopy (LRTEM) images (Figure 8). Interestingly, the morphology of P-18C6 undergoes a transformation from uniformly shaped nanovesicles of P-12C4 and P-15C5 to a necklace-type of arrangement with spherical beads which can be correlated to the increase in crown ring cavity size (12-crown-4 to 18-crown-6). Necklace type of structures, where chains of beads are connected to form elongated soft-structures were observed in P-18C6 (Figure 8). For a

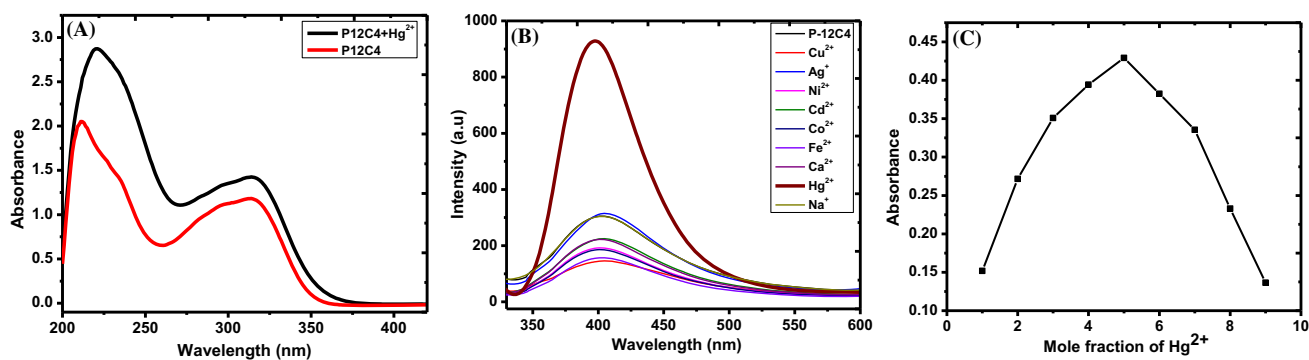


Figure 4. (a) UV-vis spectra of P-12C4 (50 μM) with Hg²⁺ ion. (b) Emission spectra with ten equivalents of perchlorate salt of different metal ions, (c) Job's plot of peptide P-12C4 showing 1:1 binding with Hg²⁺ ions.

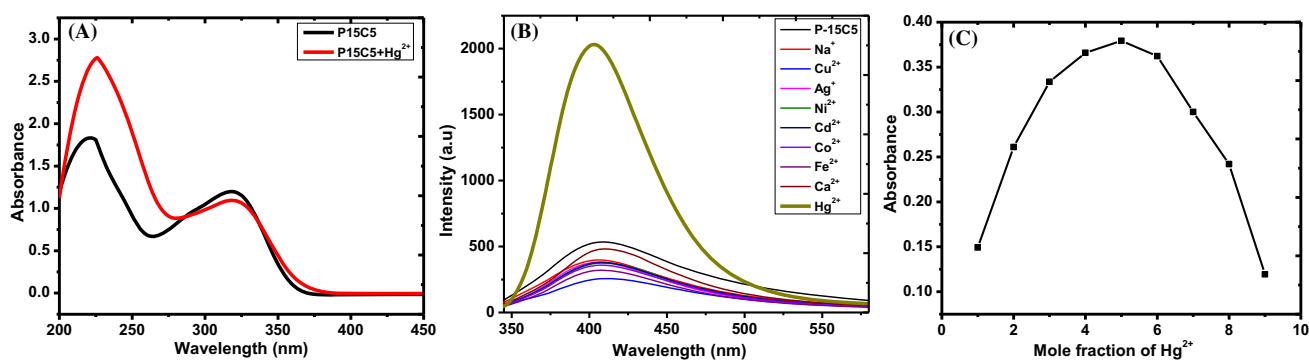


Figure 5. (a) UV-vis spectra of P-15C5 (50 μM) Hg²⁺ ion., (b) emission spectra with ten equivalents of perchlorate salt of different metal ions, (c) Job's plot of peptide P-15C5 showing 1:1 binding with Hg²⁺ ions.

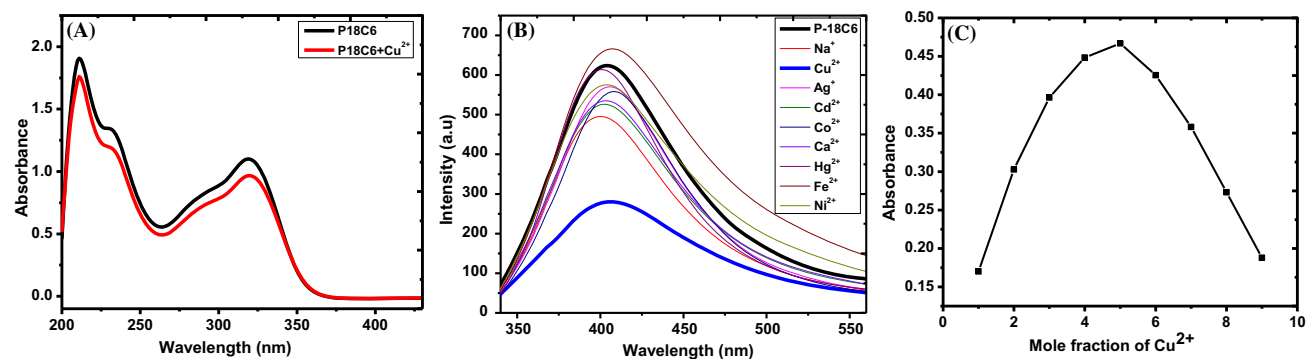


Figure 6. (a) UV-vis spectra of P-18C6 (50 μM) with Cu²⁺ ion, (b) emission spectra with ten equivalents of perchlorate salt of different metal ions, (c) Job's plot of peptide P-18C6 showing 1:1 binding with Cu²⁺ ions.

given building block of peptide molecules, its crown ring cavity size and hydrophobicity on the exterior of the ring are responsible for this transformation. LRTEM images corroborated well with the self-assembled structures observed in AFM and SEM images. Interlinked solid spheres were observed for P-12C4 and P-15C5 while a better hydrogen bonding ability of P-18C6

leads to interlinked necklace-like hollow spherical particles.

3.3a Peptide interaction with mercuric ions: Having demonstrated the formation of vesicles and selectivity of peptides P-12C4 and P-15C5 towards Hg²⁺ ion, we aged the two solutions for 12 h and studied their

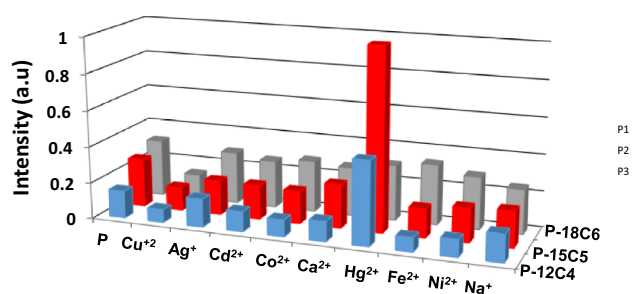


Figure 7. Comparison of emission of peptides with different metal ions in methanol at their λ_{\max} . [λ_{\max} for P-12C5 = 403 nm, for P-15C5 = 406 nm, P-18C6 = 403 nm].

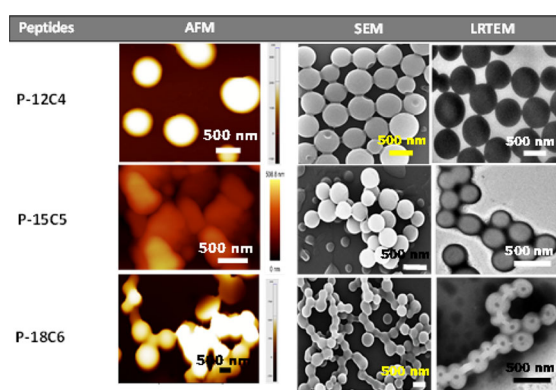


Figure 8. Comparative self-assembled morphologies of crown ether substituted peptides as seen under AFM, SEM, and LRTEM.

fluorescence response and morphologies again in the presence of Hg^{2+} ions. There was no change in the recorded fluorescence. Interaction of cations with the peptides that trigger self-assembly is a well-studied phenomenon.⁹ Moreover, mercury ions are also known to interact with the crown ether ring in the literature.¹⁰ Katerinopoulos and coworkers, recently designed a fluorescent sensor for Hg^{2+} with 7-amino-4 methylcoumarine¹¹ and monoaza-15-Crown-5. The Caos group developed a turn off sensor for mercuric ions bearing an aza-15-crown-5 as a binding unit.¹² The report of such interactions prompted us to use mercury ion as an external stimuli to study peptides self-assembly. Peptides (P-12C4 and P-15C5) formed nanovesicles on incubation with the Hg^{2+} ions in the 1:1 molar ratio. Peptides were incubated with Hg^{2+} for 12 h and displayed a disintegration of these soft structures. SEM and TEM micrographs revealed the disruption of the vesicular structure (Figures 9, 10).

3.3b Peptides with sodium ions: The affinity of crown ether for alkali and alkaline earth metals is a well-studied phenomenon that catalyzes phase transfer reactions and transports ions across lipophilic membranes. We reasoned that incubation of vesicles with alkali metal ions like sodium ion might influence the self-assembly *via* ion-dipole interactions with these cations. The known proclivity of crown ethers to form complexes with cations prompted us to use sodium ions as an external

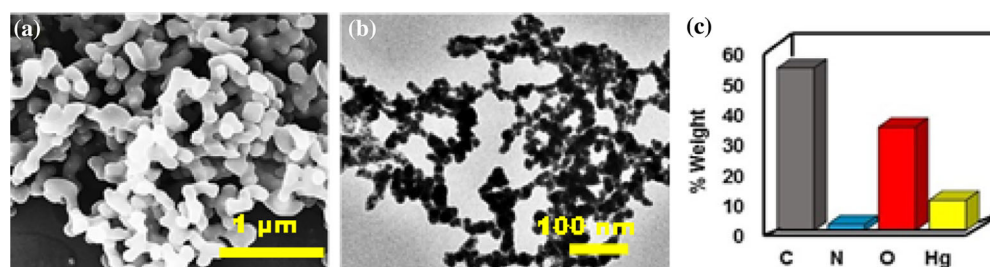


Figure 9. Microscopic images of peptide P-12C4 + Hg^{2+} complex in MeOH (a) SEM images. (b) LRTEM images (negative staining with 1% uranyl acetate). (c) EDX analysis.

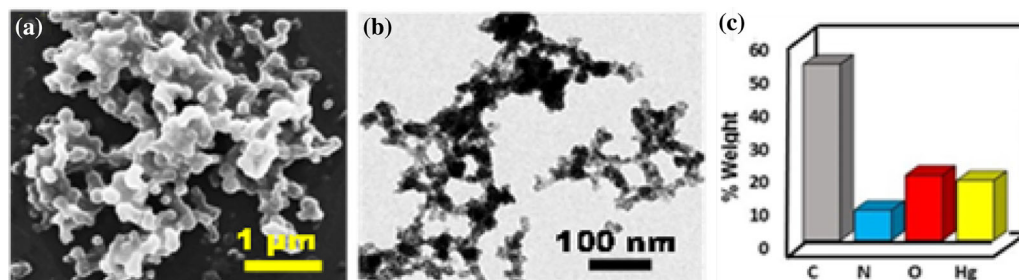


Figure 10. Microscopic images of peptide P-15C5 + Hg^{2+} complex in MeOH (a) SEM images. (b) TEM images (negative staining with 1% uranyl acetate). (c) EDX analysis.

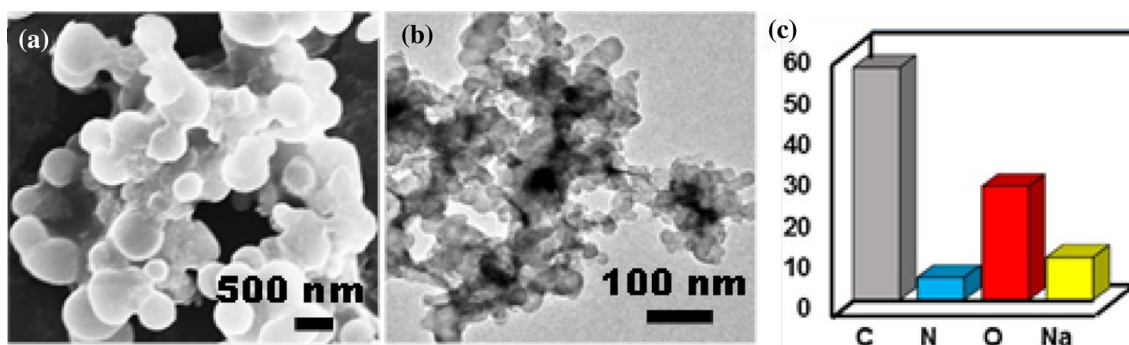


Figure 11. Microscopic images of peptide P-12C4+Na⁺ complex in MeOH (a) SEM images. (b) LRTEM images (negative staining with 1% uranyl acetate). (c) EDX analysis.

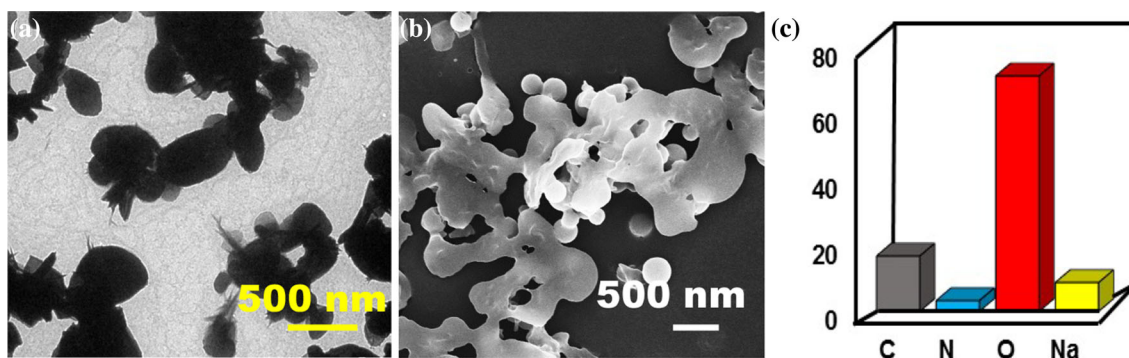


Figure 12. Microscopic images of peptide 15C5 + Na⁺ complex in MeOH (a) LRTEM images (negative staining with 1% uranyl acetate). (b) SEM images. (c) EDX analysis.

stimulus for altering peptide self-assembled structures. Interestingly, the vesicular structures ruptured after 12 h upon incubation of peptides (P-12C4, P-15C5) with perchlorate salt of sodium even at ambient temperature (Figures 11,12).

4. Conclusions

The synthesized tripeptides reported here adopt an α -helical turn type conformation in the solid state and a random coil (unordered pattern) in the solution. Interestingly, these Δ^2 Phe functionalized crown ether peptides also show a potential to form complexes with metal ions. The cation binding ability with varying crown ether ring sizes could also be studied. Notably, peptides P-12C4 and P-15C5 have shown fluorescence turn-on sensing towards Hg²⁺ ion. Microscopic studies have shown that the presence of Hg²⁺ and Na⁺ metal ions have resulted in rupturing of the well-defined nanovesicles in these peptides.

Supplementary Information (SI)

Synthesis of peptides, UV and fluorescence data, FT-IR, CD spectra and ¹H and ¹³C NMR spectra of peptides are included

in the supplementary information available at www.ias.ac.in/chemsci.

Acknowledgements

KT thanks the Council of Scientific and industrial research (India) for a junior and senior research fellowship.

Compliance with ethical standards

Conflict of interest There are no conflicts to declare.

References

- Samorí P, Engelkamp H, Witte P D, Rowan A E, Nolte R J M and Rabe J P 2001 Self-assembly and manipulation of crown ether phthalocyanines at the gel-graphite interface *Angew. Chem. Int. Ed.* **40** 2348
- (a) Biron E, Voyer N, Meillon J C, Cormier M E and Auger M 2000 Conformational and orientation studies of artificial ion channels incorporated into lipid bilayers *Biopolymers* **55** 364; (b) Voyer N and Robitaille M 1995 A novel functional artificial ion channel *J. Am. Chem. Soc.* **117** 6599
- (a) Dinesh B, Squillaci M A, Ménard-Moyon C, Samorí P and Bianco A 2015 Self-assembly of diphenylalanine

- backbone homologs and their combination with functionalized carbon nanotubes *Nanoscale* **7** 15873; (b) Marchesan S, Vargiu A V and Styan K E 2015 The Phe-Phe motif for peptide self-assembly in nanomedicine *Molecules* **20** 19775; (c) Nguyen V, Zhu R, Jenkins K and Yang R 2016 Self-assembly of diphenylalanine peptide with controlled polarization for power generation *Nat. Commun.* **7** 13566
- (a) Fukuda R, Takenaka S and Takagi M 1990 Metal ion assisted DNA-intercalation of crown ether-linked acridine derivatives *J. Chem. Soc. Chem. Commun.* **0** 1028; (b) Hall A C, Suarez C, Hom-Choudhury A, Manu A N A, Hall C D, Kirkovits G J, Ghiriviga I and Velmurugan D 2003 Cation transport by a redox-active synthetic ion channel *Org. Biomol. Chem.* **1** 2973; (c) Lopes J L, Miles A J, Whitmore L and Wallace B A 2014 Distinct circular dichroism spectroscopic signatures of polyproline II and unordered secondary structures: applications in secondary structure analyses *Protein Sci.* **23** 1765
 - (a) Elizarov A M, Chang T, Chiu S-H and Stoddart J F 2002 Self-Assembly of dendrimers by slippage *Org. Lett.* **4** 3565; (b) Gokel G W, Leevy W M and Weber M E 2004 Crown ethers: sensors for ions and molecular scaffolds for materials and biological models *Chem. Rev.* **104** 2723
 - Uma K, Karle I L and Balam P 1991 Towards the design of structural mimics for proteins using helical peptide modules in *Proteins: Structure, Dynamics and Design* V Renugopalakrishnan, P R Carey, I C P Smith, S G Huang and A Storer (Eds.) (Netherlands: Escom Science Publishers) pp. 295–301
 - (a) Lopes J L, Miles A J, Whitmore L and Wallace B A 2014 Distinct circular dichroism spectroscopic signatures of polyproline II and unordered secondary structures: applications in secondary structure analyses *Protein Sci.* **23** 1765; (b) Saini A and Chauhan V S 2014 Self-assembling properties of peptides derived from TDP-43 C-terminal fragment *Langmuir* **30** 3845
 - (a) Kar S and Tai Y 2015 Marked difference in self-assembly, morphology, and cell viability of positional isomeric dipeptides generated by reversal of sequence *Soft Matter* **11** 1345; (b) Mishra A and Chauhan V S 2011 Probing the role of aromaticity in the design of dipeptide based nanostructures *Nanoscale* **3** 945; (c) Panda J J, Mishra A, Basu A and Chauhan V S 2008 Stimuli-responsive self-assembled hydrogel of a low molecular weight free dipeptide with potential for tunable drug delivery *Biomacromolecules* **9** 2244; (d) Panda J J and Chauhan V S 2014 Short peptide-based self-assembled nanostructures: implications in drug delivery and tissue engineering *Polym. Chem.* **5** 4418; (f) Wang Q, Yu J, Zhang X, Liu D, Zheng J, Pan Y and Lin Y 2013 Controlled biosilification using self-assembled short peptides A₆K and V₆K *RSC Adv.* **3** 2784; (g) Wang Q, Yu J, Zheng J, Liu D, Jiang F, Zhang X and Lib W 2013 Morphology-controlled synthesis of silica materials templated by self-assembled short amphiphilic peptides *RSC Adv.* **3** 15955
 - (a) Liu S, Zhao L, Xiao Y, Huang T, Li J, Huang J and Yan Y 2016 Allosteric in molecular self-assemblies: metal ions triggered self-assembly and emissions of terthiophene *ChemComm* **52** 4876; (b) Mondal S, Swaroop S, Gurunath R and Verma S 2010 A synthetic ditryptophan conjugate that rescues bacteria from mercury toxicity through complexation *Tetrahedron Lett.* **51** 6111
 - (a) Dai H, Liu F, Gao Q, Fu T and Kou X 2011 A highly selective fluorescent sensor for mercury ion (II) based on azathia-crown ether possessing a dansyl moiety *Luminescence* **26** 523; (b) Yan Z, Hu L, Nie L and Lu H 2011 Preparation of 4,4'-bis-(carboxyl phenylazo)-dibenzo-18-crown-6 dye and its application on ratiometric colorimetric recognition to Hg²⁺ *Spectrochim. Acta A* **79** 661
 - Voutsadaki S, Tsikalas G K, Klontzas E, Froudakis G E and Katerinopoulos H E 2010 A “turn-on” coumarin-based fluorescent sensor with high selectivity for mercury ions in aqueous media *ChemComm* **46** 3292
 - Hou C, Urbanec A M and Cao H 2011 A rapid Hg²⁺ sensor based on aza-15-crown-5 ether functionalized 1,8-naphthalimide *Tetrahedron Lett.* **52** 4903